Title: ^{2}H-fractionations during the biosynthesis of carbohydrates and lipids imprint a metabolic signal on the δ^{2}H values of plant organic compounds

Authors: Cormier M-A.[a,b,*], Werner R. A.[a], Sauer P. E.[c], Gröcke D. R.[d], Leuenberger M. C.[e], Wieloch T.[f], Schleucher J.[f] and Kahmen A.[b]

Affiliations:

[a]ETH Zürich, Department of Environmental Systems Science, Universitätstrasse 2, 8092 Zürich, Switzerland.

[b]University of Basel, Department of Environmental Sciences - Botany, Schönbeinstrasse 6, 4056 Basel, Switzerland.

[c]Department of Geological Sciences, Indiana University, Bloomington, IN 47405-1405, USA.

[d]Stable Isotope Biogeochemistry Laboratory, Durham University, Science Laboratories, South Road, Durham, DH1 3LE, UK.

[e]Climate and Environmental Physics, Physics Institute and Oeschger Centre for Climate Change Research, University of Bern, Bern, Switzerland

[f]Department of Medical Biochemistry and Biophysics, Umeå University, 901 87 Umeå, Sweden.

[*]Corresponding author: marc-andre.cormier@usys.ethz.ch

Keywords: alkanes, cellulose, biomarker, hydrogen isotopes, plant metabolism

Abstract

- δ^2H analyses of plant organic compounds have been applied to assess ecohydrological processes in the environment despite a large part of the δ^2H variability observed in plant compounds not being fully elucidated.

- We present a new conceptual biochemical model based on empirical H isotope data that we generated in two complementary experiments that explains where ^2H-fractionations occur in the biosynthesis of plant organic compounds and how these ^2H-fractionations are tightly coupled to a plant's carbon and energy metabolism.

- With this work, we demonstrate that information recorded in the δ^2H values of plant organic compounds goes beyond hydrological signals and can also contain important information on the carbon and energy metabolism of plants. As such we provide a mechanistic basis to introduce hydrogen isotopes in plant organic compounds as new metabolic proxy for the carbon and energy metabolism of plants and ecosystems. Such a new metabolic proxy has the potential to be applied in a broad range of disciplines, including plant and ecosystem physiology, biogeochemistry and paleoecology.

Introduction

The analyses of stable isotope ratios in plant material have proven to be an indispensable tool for ecological, biogeochemical and (paleo-) climatological research (Dawson et al., 2002). Of the four most common biogenic elements, only carbon (C), oxygen (O), and nitrogen (N) isotope ratios of plant compounds are fully established as proxies for different ecological, environmental and paleoclimatological processes. In contrast, hydrogen (H) isotope ratios in plant compounds are less commonly applied. New developments in isotope-ratio mass spectrometry for compound-specific analyses (Burgoyne & Hayes, 1998), e.g. of leaf wax lipids, and new equilibration methods (Filot et al., 2006) have, however, promoted the use of H isotopes in recent years. In particular, H isotope analyses of biomarkers such as leaf waxes have been successfully applied in paleohydrological research over the past decade and have highlighted the tremendous potential of hydrogen isotope ratios in plant-derived compounds for ecological, environmental and paleoclimatological research (Sachse et al., 2012).

Three main drivers that have been identified to determine the H isotope composition (δ^2H) in plant organic compounds are: (i) δ^2H of the plant's water source (Chikaraishi & Naraoka, 2003; Sachse *et al.*, 2006; Hou *et al.*, 2008), (ii) leaf water evaporative ^2H-enrichment, which is largely driven by the evaporative environment of the plant (Smith & Freeman, 2006; Feakins & Sessions, 2010a; Kahmen *et al.*, 2013a,b), and (iii) biosynthetic ^2H-fractionation (^2H-ε_{bio}), which includes several different biochemical processes and corresponds to the ^2H-fractionation between the biosynthetic cellular water pool and the organic compounds (Ziegler *et al.*, 1976; Sternberg *et al.*, 1984b; Ziegler, 1989; Yakir & DeNiro, 1990; Luo & Sternberg, 1992; Yakir, 1992; Schmidt *et al.*, 2003).

Most biogeochemical and paleohydrological studies that have applied stable H isotopes in plant-derived biomarkers have considered ^2H-ε_{bio} for any given compound to be constant within a species (e.g. Sachse *et al.*, 2004; 2006). As such, δ^2H values in plant organic compounds are assumed to be mainly influenced by the plant's source water δ^2H values and the evaporative ^2H-enrichment of leaf water (i.e. Rach et al., 2014). The δ^2H values of e.g. leaf wax *n*-alkanes are thus increasingly applied as proxy for (paleo-) hydrological processes (Sachse et al., 2012). However, there are indications that ^2H-

ε_{bio} can vary for a given compound within a species and that this variability is related to the C metabolism of the plant (Ziegler *et al.*, 1976; Estep & Hoering, 1980; Yakir & DeNiro, 1990; Luo & Sternberg, 1992; Schmidt *et al.*, 2003; Liu & Huang, 2008; Pedentchouk *et al.*, 2008). It has been suggested that photosynthetic H isotope fractionation processes during the reduction of NADPH in the light reaction of photosynthesis and the primary assimilation of triose phosphates, and particularly post-photosynthetic ^{2}H-fractionation processes, which correspond to all other reactions following this primary assimilation, determine $^2\text{H-}\varepsilon_{bio}$ in plants (Roden et al., 2000). A comprehensive understanding of how variations in photosynthetic and post-photosynthetic biochemical processes determine ^{2}H-fractionation during compound biosynthesis in plants does, however, not exist.

Here, we present new empirical data and a conceptual biochemical model that highlights how and where ^{2}H-fractionation occurs during photosynthetic and post-photosynthetic processes in plants. The conceptual model is designed to mechanistically understand different magnitudes in $^2\text{H-}\varepsilon_{bio}$ in different plant-derived organic compound classes and to link the variability of $^2\text{H-}\varepsilon_{bio}$ within a given compound to metabolic processes in plants. As such, our model will provide new opportunities for the interpretation of δ^2H values in plant-derived organic compounds and will in particular facilitate the use of δ^2H values in plant-derived compounds to assess processes related to the carbon metabolism of plants.

We build our model on empirical H isotope data that we generated in two complementary experiments. In both experiments we tested the effects of the plants carbon metabolism on the hydrogen isotope composition of plant-derived carbohydrates and lipids by experimentally manipulating the photosynthetic carbohydrate supply to the plant. In the first experiment, we manipulated the photosynthetic carbohydrate supply to plants by limiting the CO_2 that is available for the dark reaction of photosynthesis. Specifically, we grew six different vascular plant species under four different atmospheric CO_2 concentrations (pCO_2) stretching from estimated glacial maximum conditions (Tripati et al., 2009) and above the photosynthetic CO_2 compensation point (Krenzer & Moss, 1969; Kestler *et al.*, 1975; Gerhart & Ward, 2010) to the averaged 2100 forecasts (Stocker et al., 2013) (i.e. 150, 280, 400 and 800 ppm). In the second experiment, we manipulated the photosynthetic

carbohydrate supply to plants by limiting the light reaction of photosynthesis and forced the plants to meet their carbohydrate demands from reserves such as starch. For this purpose, we grew six different vascular plant species, which exhibit an autotrophic carbon metabolism when grown under natural environmental conditions, from bulbs, large seeds or tubers, that contain large carbohydrate reserves for 12 weeks under four different light treatments (0, 8, 115 and 355 µmol photons m^{-2} s^{-1}).

While all H atoms in plant-derived organic compounds originate from water, photosynthetic and post-photosynthetic H isotope fractionation in plants strongly depend on the biochemical origin of H atoms during biosynthesis (Fig. 1). Three biochemical origins of H in plants are important in this respect: (i) The organic precursor molecules in a biosynthetic pathway, e.g. the H atoms of ribulose-1,5-bisphosphate that are transferred to the 2 triose phosphates (TP) synthesized in the Calvin cycle or the acetyl-CoA hydrogens in the fatty acid biosynthetic pathway (Sachse et al., 2012). (ii) Redox cofactors, e.g. the biological reducing agent nicotinamide adenine dinucleotide phosphate (NADPH), that provide an important part of the H atoms in organic compounds (Kazuki et al., 1980). (iii) The cellular water, which is incorporated into organic molecules either by H addition to sp^2 hybrized-C atoms (i.e. C=C), for example by the fumarase reaction in the TCA cycle (Blanchard & Cleland, 1980), or by (partial) exchange of C-bound H atoms in CH_2-groups adjacent to CO-groups e.g. by the triosephosphate isomerase via an enolic structure in the glycolysis (Maister et al., 1976).

To identify for our model how changes in the plant's carbon metabolism affect the biochemical origin of H in photosynthetic and post-photosynthetic biochemical processes, we analysed in our experiments the δ^2H values of two different compound classes that differ in their biochemical pathways and thus in the contribution of H from different biochemical origins in their biosynthesis. These compound classes are carbohydrates (i.e. α-cellulose) and lipids (i.e. *n*-alkanes).

Materials & methods

CO_2 experiment: In four climate controlled greenhouses, we grew six different C_3 plant species from seeds (i.e. two grasses: *Arrhenatherum elatius* and *Festuca rubra*; two legumes: *Trifolium pratense* and *Lathyrus pratensis*; two forbs: *Centaurea jacea* and *Plantago lanceolate*) under four atmospheric CO_2 concentrations (150, 280, 400 and 800 ppm). All the other parameters have been kept constant during the experiment (T = 20°C during day and 10°C during night, rH = 60%, LD 14:10 cycle). Plants were grown in 3 replicates. After 12 weeks, the plants were harvested and oven-dried at 50°C. Leaves were sampled at five different days during the growing experiments for leaf water extractions and conserved frozen in Exetainer vials (gas tight).

Light experiment: In four climate controlled growth chambers, four different light treatments (0, 8, 115 and 355 µmol photons m^{-2} s^{-1}) were constantly applied on six different plant species (i.e. C_3 species: S*olanum tuberosum, Ipomoea* sp., *Helianthus tuberosus, Zingiber officinale, Allium cepa*, and finally *Zea mays* subsp. *Mays*, a C_4 plant), while the other parameters were kept constant (T = 25°C, rH = 60%). Plants were grown in four replicates mostly from large storage organs (i.e. tubers for S*olanum tuberosum, Ipomoea* sp., and *Helianthus tuberosus*, roots for *Zingiber officinale*, bulb for *Allium cepa,* and seeds for *Zea mays* subsp. *mays*) in the dark and low light treatments. After 12 weeks of growing, the plants were harvested and oven-dried at 50°C. Leaves were sampled at 11 different days during the growing experiments for leaf water extractions and conserved frozen in Exetainer vials. The environmental variables for the light and the CO_2 experiments are summarized in the tables S3 and S4.

Chemical purifications: For all specimens, leaf wax *n*-alkanes and α-cellulose were extracted and purified from the dried plant material. The lipids (including *n*-alkanes) were extracted in combusted glass vials from 1 g of dry leaves using 30 mL of a dichloromethane (DCM) : methanol mixture (9:1) under an ultrasonic bath during 15 min. Hydrocarbons (including *n*-alkanes) were subsequently isolated for isotope analysis from other lipids by column chromatography by eluting 10 mL hexane in 6 mL combusted glass silica-gel columns. The columns were pre-prepared by filling about three quarters (i.e. 2 g) of the column volume with silica-gel (0.040-0.063 mm, 99.5% pure). The columns were rinsed with 10 mL acetone, 10 mL DCM and 10 mL hexane and finally chemically activated in a desiccation oven at 60°C over-night. The

other lipids, including sterols and fatty acids, were eluted after the *n*-alkanes with a DCM : methanol mixture (9:1) and preserved for future analyses. For more details on the method see Peters *et al.* (2005).

For H isotope analyses on α-cellulose, the cellulose was purified according to the method presented by Gaudinski *et al.* (2005). Briefly, about 150 mg of dry leaves was washed off from all lipids in Ankom bags by reflux in a Soxhlet apparatus with a toluene: ethanol (95%) mixture (2:1) for about 24 hrs under high heat, and then under ethanol only, until the solvent in the Soxhlet chamber was clear. Following this lipid removal, lignin was oxidised and washed away from the samples with a bleaching solution of sodium chloride and acetic acid (pH 4) under ultrasonic bath at 70°C for about 24 hrs. Finally, the α-cellulose was purified from holocellulose with a 15% NaOH cold solution also under ultrasonic bath.

All plant-extractable leaf water was quantitatively extracted on a cryogenic water extraction line as described in West *et al.* (2006) and analyzed for its δ^2H values (see tables S1 and S2). The frequent leaf water monitoring throughout both experiments allowed us to deduce an accurate ^{2}H-ε_{bio} for *n*-alkanes and α-cellulose excluding the effect of leaf water evaporative ^{2}H-enrichment as:

Eq. 1. $^{2}H - \varepsilon_{bio} = (1000 \cdot (organic\ compound\ \delta^{2}H + 1000\ )/(leaf\ water\ \delta^{2}H + 1000\ ) - 1))$

Even though heterogeneity in leaf water δ^2H exists (Cernusak *et al.*, 2016), we used the mean bulk leaf δ^2H water to calculate ^{2}H-ε_{bio} since sub-cellular leaf water δ^2H values cannot be measured and we did not want to add additional uncertainties into our empirical data by modelling them. We decided – as typically done in the literature – to calculate the ^{2}H-ε_{bio} as the difference between mean bulk foliar water (measured several times during the experiment) and the organic δ^2H values (measured at the end of the experiment).

While homologous *n*-alkanes δ^2H values can vary, even within a single plant (e.g. Chikaraishi & Naraoka, 2003; Magill *et al.*, 2013), we measured δ^2H values of the C29 *n*-alkane as it was the only compound abundant enough for GC-IRMS measurements that occurred in all species. To allow the comparison of treatment effects on ^{2}H-ε_{bio}

across all six species, we standardized the ^{2}H-ε_{bio} response of a species to its overall mean ^{2}H-ε_{bio} in both experiments (i.e. Δ^2H-ε_{bio}).

Isotope analyses: The water δ^2H values have been measured on a DeltaPlus XP isotope ratio mass spectrometer (IRMS) coupled to a high temperature conversion elemental analyzer (TC/EA) via a conFloIII (Gehre *et al.*, 2004). Following the method described by Sessions (2006), δ^2H values on *n*-alkanes have been measured on a second Delta V plus stable isotope ratio mass spectrometer (IRMS) coupled to a Trace GC Ultra and a GC Isolink via a ConFlow IV. The cellulose δ^2H values of the non-exchangeable H atoms were measured following an equilibration of the exchangeable H atoms as described by Schimmelmann (1991), Filot *et al.* (2006) and Sauer *et al.* (2009) using a TC/EA coupled to a Delta Advantage IRMS.

Data analyses: We fitted hyperbolic functions (expressing the balance between photosynthetic and post-photosynthetic effects on Δ^2H-ε_{bio}) enhanced with linear functions (expressing the possible influence of photorespiration (Ehlers *et al.*, 2015)) into the relationships between the independent variables we manipulated in the two experiments and Δ^2H-ε_{bio}: $\delta^2H = a + b/x + c \cdot d \cdot x/(c \cdot x + d)$, were x is either the light intensity or the pCO_2 values and a to d represent model-calculated parameters. At the positive end, the photosynthetic processes dominate and the inputs of new assimilates and light derived NADPH are at a maximum value and drive Δ^2H-ε_{bio} towards negative values. At the negative end, the pool of photosynthetic carbohydrate supply is low, due to little amount of, or no, new assimilates, resulting in an infinite cycling of individual compounds in this pool and driving toward positive values of Δ^2H-ε_{bio}.

Results and discussion

Both, the CO_2 and light limitation experiments revealed that ^{2}H-ε_{bio} varied systematically in different compound classes in response to the photosynthetic carbohydrate supply. This indicates that changes in plant C metabolism have strong effects on ^{2}H-fractionation during the biosynthesis of organic compounds in plants (Figs. 2 and 3).

In the first experiment, we found strong effects of pCO_2 on leaf water evaporative ^2H-enrichment in all six CO_2 treated plants (Fig. 2a). The effects of pCO_2 on leaf water δ^2H values can be explained by the CO_2 sensitivity of stomatal conductance and resulting effects on the evaporative ^2H-enrichment of leaf water. In the Péclet-modified Craig-Gordon model, transpiration has been shown to reduce ^2H-enrichment of leaf water due to the dilution of leaf water with unenriched source water (Cernusak et al., 2016). The increase in leaf water δ^2H values at higher pCO_2 that we observed in our experiment can therefore be explained by reduced stomatal conductance and transpiration, resulting in a decreased Péclet effect. δ^2H values differed strongly between α-cellulose and *n*-alkanes and showed no unidirectional relationship with pCO_2 (Fig. 2b, d). Importantly, when the effects of leaf water evaporative ^2H-enrichment on δ^2H values of α-cellulose and *n*-alkanes were accounted for by subtracting leaf water δ^2H values from δ^2H values of organic compounds (and calculating as such ^2H-ε_{bio} for a given compound class and species using Eq. 1), we observed that the ^2H-ε_{bio} for α-cellulose and *n*-alkanes was strongly affected by pCO_2 in all six species (Fig. S1). When the inherent species specific variability in ^2H-ε_{bio} was accounted for by standardizing the treatment response of ^2H-ε_{bio} for a given compound around the overall mean ^2H-ε_{bio} of a species (i.e. calculating Δ^2H-ε_{bio}), it became evident that the pCO_2 effects on ^2H-ε_{bio} were consistent in trend and magnitude across all species and for both compound classes (Fig. 2c, e). Effects were strongest at the lowest pCO_2 level, where we assume that the plant's carbon metabolism became limited by photosynthetic carbohydrate supply (Drake et al., 1997). For both α-cellulose and *n*-alkanes, ^2H-ε_{bio} at 150 ppm was 20‰ and 16‰ more positive (at probability $p<0.05$ and $p<0.001$, respectively, using F-values from two-way ANOVA) than at pre-industrial pCO_2 (i.e. 280 ppm). However, ^2H-ε_{bio} did not become increasingly negative beyond 400 ppm pCO_2.

In the second experiment, we found strong effects of the available photosynthetically active radiation (PhAR) on leaf water evaporative ^2H-enrichment in all six plant species (Fig. 3a). The effects of light intensity on leaf water δ^2H values can be explained by the light sensitivity of stomatal conductance and resulting effects on the evaporative ^2H-enrichment of the leaf water (Cernusak et al., 2016). δ^2H values differed strongly between α-cellulose and *n*-alkanes and δ^2H values of both compounds showed a

292 negative relationship with increasing PhAR (Fig. 3b, d). When the effects of leaf water
293 evaporative ^{2}H-enrichment were accounted for by subtracting leaf water δ^2H values
294 from δ^2H values of organic compounds, we found that ε_{bio} for α-cellulose and *n*-alkanes
295 was strongly affected by light intensity in all six species (Fig. S2). The effect was
296 greatest under fully dark conditions, when plants were completely limited in their
297 photosynthetic carbohydrate supply and were forced to meet 100% of their carbon and
298 energy demands from carbohydrate reserves or other organic molecules (i.e. sugars,
299 proteins, lipids). When ^{2}H-ε_{bio} responses were standardized (i.e. Δ^2H-ε_{bio}) across
300 species to allow comparison of the treatment effects across species, we detected that
301 the treatment responses in Δ^2H-ε_{bio} were remarkably consistent in direction and
302 magnitude across species but differed in magnitude between the two compound classes
303 (Fig 3c, e). In full dark, Δ^2H-ε_{bio} for α-cellulose and *n*-alkanes was more positive than
304 Δ^2H-ε_{bio} of plants that grew under light (Fig. 3c, e). For α-cellulose and *n*-alkanes,
305 Δ^2H-ε_{bio} at 0 PhAR was 22‰ and 43‰ more positive ($p<0.05$ and $p<0.001$,
306 respectively) than at higher PhAR (i.e. 354 µmol m^{-2} s^{-1}). However, ^{2}H-ε_{bio} did not
307 become increasingly negative beyond 115 µmol m^{-2} s^{-1} in either compound class.
308
309 Yakir & DeNiro (1990) and later Luo & Sternberg (1992) have previously shown that
310 cellulose δ^2H values increase when a plant's carbon metabolism was forced into a state
311 of low photosynthetic carbohydrate supply. We show here, that these effects are
312 relevant not only for cellulose but also for other compound classes such as lipids but
313 that the magnitude by which the plant's carbon metabolism affects ^{2}H-ε_{bio} differed for
314 compound classes and was dependent on the treatment (Figs. 2 and 3). This indicates
315 that different biochemical ^{2}H-fractionation processes determine not only ^{2}H-ε_{bio} in
316 different compound classes but that these different biochemical ^{2}H-fractionation
317 processes are differently affected by changes in the plant's carbon metabolism. This in
318 turn provides us with the opportunity to establish - based on the known biochemical
319 pathways - a conceptual biochemical model that identifies how and where H isotope
320 fractionations occur during the biosynthesis of different plant compounds and to
321 conceptualize how changes in a plant's carbon metabolism affect the ^{2}H-fractionations
322 for a given compound (Fig. 4).
323

Photosynthetic ^{2}H-fractionation: Photosynthetic ^{2}H-fractionation occurs in the chloroplast during the light reaction of photosynthesis where ferredoxin-NADP$^+$ reductase produces NADPH with reduced H that is strongly ^{2}H-depleted compared to leaf water (Luo et al., 1991). This ^{2}H-depleted H pool in NADPH is subsequently introduced into organic compounds in the Calvin cycle to form a glyceraldehyde-3-phosphate (GAP) that will be ^{2}H-depleted compared to leaf water and form a major constituent of the triosephosphate (TP) pool (Fig. 4). To our knowledge, the only attempt to estimate the magnitude of photosynthetic ^{2}H-fractionation was by Yakir & DeNiro (1990), who calculated a value of -171‰ for cellulose in the aquatic plant *Lemna gibba*. While our experiments were not designed to isolate the magnitude of the photosynthetic component of ^{2}H-ε_{bio}, we found that variations in PhAR above 115 µmol m^{-2} s^{-1} did not affect ^{2}H-ε_{bio} of α-cellulose and *n*-alkanes in any of the six species that we investigated. This is the case even though net photosynthetic rates increased with increasing light intensity in all species (Fig S3). We thus conclude that photosynthetic ^{2}H-fractionation is, for the light spectrum tested, independent of the rate of photosynthesis within a species and possibly stable for any given species. This finding is important as it suggests that variations in ^{2}H-ε_{bio} in response to plant metabolic changes observed in this study are mainly the result of variations in post-photosynthetic H isotope fractionations.

Effects of post-photosynthetic ^{2}H-fractionation on δ^2H values of different compound classes: Irrespective of the treatment, we found α-cellulose in both experiments to be less ^{2}H-depleted compared to leaf water than lipids (Figs. 2 and 3). This was for all species when these were grown at sufficient photosynthetic carbohydrate supply rates, i.e. at $pCO_2 \geq 280$ ppm or a light intensity of ≥ 8 µmol photon m^{-2} s^{-1}. This is consistent with previous studies that have reported similar patterns for cellulose or starch (Epstein *et al.*, 1976; Sternberg *et al.*, 1984a). Given the strong ^{2}H-depletion during photosynthetic H isotopes fractionation processes (Yakir & DeNiro, 1990), these values suggest that post-photosynthetic ^{2}H-fractionations have a strong effect on the observed δ^2H values of carbohydrates in plants.

Post-photosynthetic ^{2}H-enrichment commences in the TP pool that is in rapid reciprocal exchange with the hexosephosphate (HP) pool in a futile cycle from which

carbohydrates are synthesized (Buchanan et al., 2015) (Fig. 4). Several processes can lead to the post-photosynthetic ^{2}H-enrichment of the TP and HP pools as outlined in our conceptual model (Fig. 1 and 4): (i) The synthesis of GAP in the Calvin cycle allows (partial) exchange of C-bound H atoms with the surrounding (^{2}H-enriched) cellular water in CH_2-groups adjacent to CO-groups via an enolic structure (Rieder & Rose, 1959; Maister *et al.*, 1976; Knowles & Albery, 1977), leading to an ^{2}H-enrichment of the GAP pool. Wang *et al.* (2009) have calculated a theoretical equilibrium fractionation of organic H for H-C-OH positions up to 96‰, illustrating that C-bound H exchange with water can drive GAP and consequently carbohydrates towards positive δ^2H values. (ii) In new photosynthetically derived GAP, only one out of four C-bound H atoms is derived from ^{2}H-depleted NADPH from the light reaction of photosynthesis. The other C-bound H atoms are coming from the precursor molecule 3-phosphoglyceraldehyde (3-PGA) that is ^{2}H-enriched compared to NADPH because of previous H exchanges with cellular water as described above. (iii) During the production of HP, where two trioses are bound to form fructose 1,6-bisphosphate, one out of four C-bound H atoms is lost to the surrounding water (Rose & Rieder, 1958; Hall *et al.*, 1999). As light isotopologues will react faster in this reaction, this process leads to a ^{2}H-enrichment of the GAP pool (Schmidt et al., 2015). (iv) The enzyme phosphoglucose isomerase used to interconvert glucose 6-phosphate and fructose 6-phosphate might ^{2}H-enrich the HP pool even further during that step by allowing partial exchange of specific H atoms (Fig. 1) with the surrounding cellular water (Schleucher et al., 1999).

As a consequence of the different post-photosynthetic ^{2}H-fractionation processes that lead to a ^{2}H-enrichment of the TP and the HP pool, carbohydrates typically do not deviate as strongly in their δ^2H values from leaf water as we would expect from the primary ^{2}H-depletion of the NADPH pool that is generated in the light reaction of photosynthesis. While the above-described mechanisms are relevant for all carbohydrates, δ^2H values can vary among different carbohydrates. Previous studies have for example shown that starch is ^{2}H-depleted compared to cellulose (Smith & Epstein, 1970; Luo & Sternberg, 1991) and compared to leaf soluble sugars (Schleucher et al., 1999). This has been attributed to a ^{2}H-depletion at position C2 caused by the pronounced disequilibrium of phosphoglucose isomerase (Schleucher et al., 1999). Analogous ^{3}H-depletion at the same position was found by Dorrer *et al.* (1966).

n-Alkanes and lipids in general had more negative ^{2}H-ε_{bio} than α-cellulose in our and in previous studies (Smith & Epstein, 1970; White, 1989; Schmidt *et al.*, 2003). This is despite the fact that the precursor molecule in lipid biosynthesis, phosphoenolpyruvate (PEP) and eventually acetyl-CoA, are originating from the same ^{2}H-enriched TP pools, as the precursor molecules of carbohydrates (Buchanan et al., 2015). In addition, the metabolic conversion of GAP to organic acids (i.e. PEP, pyruvate and malate) and from organic acids to acetyl-CoA involves the loss of ^{2}H-depleted H to nicotinamide adenine dinucleotide (NADH) and NADPH during glycolysis and loss of ^{2}H-depleted hydrogen in form of NADH, flavin adenine dinucleotide ($FADH_2$), and in some cases NADPH, that occurs in the tricarboxylic acid (TCA) cycle (Rambeck & Bassham, 1973; Møller & Rasmusson, 1998; Igamberdiev & Gardeström, 2003; White *et al.*, 2012). Also, during the conversion of organic acids to acetyl-CoA and in the TCA cycle exchange of C-bound H atoms with surrounding ^{2}H-enriched water occurs (Rambeck & Bassham, 1973; Silverman, 2002; Allen *et al.*, 2015). Organic acids as the precursor molecules of lipids should thus be more ^{2}H-enriched than molecules in the TP pool. This is, however, not reflected in lipids because ^{2}H-depleted NADPH is a critical source of H in their biosynthesis. In carbohydrates, approximately 15% of C-bound H atoms originate from ^{2}H-depleted NADPH that is produced during the light reaction of photosynthesis in the chloroplast and by the oxPPP in the cytosol (Fig. 1). In contrast, about half of the C-bound H atoms originate from ^{2}H-depleted NADPH in the autotrophic fatty acid and *n*-alkane biosynthesis (Kazuki et al., 1980; Baillif et al., 2009) (Fig. 5). As such, lipids in general and *n*-alkanes in particular are strongly ^{2}H-depleted compared to carbohydrates in autotrophically growing plants.

Metabolic effects on post-photosynthetic ^{2}H-fractionation: Our experiments revealed that plants that were forced into a state of low photosynthetic carbohydrate supply, whether by light or by CO_2 limitation, have ^{2}H-ε_{bio} values for α-cellulose and *n*-alkanes that are significantly less negative than those of plants growing under higher photosynthetic carbohydrate supply. The general trend of this effect was consistent in the two experiments and suggests that the post-photosynthetic ^{2}H-fractionation processes described in detail below lead to more positive δ^2H values when plants operate in a state of low photosynthetic carbohydrate supply (Luo & Sternberg, 1992; Yakir, 1992).

We identified two important post-photosynthetic biochemical processes that are responsible for the general ^{2}H-enrichment of plant metabolites under low photosynthetic carbohydrate supply (see Fig. 4).

(I) We assume that a substrate-limited Calvin cycle as induced by our two experiments results in smaller TP and HP pools and consequently a higher turnover of the individual molecules in a pool at a given metabolic rate. We suggest that higher turnover rates of individual molecules in the TP and HP pools lead to increasing ^{2}H-enrichment because the likelihood of equilibrium exchange of C-bound H in the TP and HP molecules with ^{2}H-enriched cellular water increases (Luo & Sternberg, 1992; Augusti *et al.*, 2006). Similar processes have been suggested for the exchange of O atoms during the biosynthesis of cellulose (Yakir & DeNiro, 1990; Hill *et al.*, 1995; Sternberg *et al.*, 2003; Barbour, 2007). While two out of six C-bound H atoms on a glucose-6-phosphate (i.e. C2 & C3) are always exchanged with the surrounding cellular water during the biosynthesis from ribusole-1,5-bisphosphate, the two C-bound H atoms on position C4 and C5 are only partially exchanged with the surrounding water (Rose & Rieder, 1958; Rieder & Rose, 1959; Fiedler *et al.*, 1967; Maister *et al.*, 1976; Knowles & Albery, 1977) (Fig. 1). A higher cycling rate of these molecules increases thus the chance for equilibration to happen on positions C4 and C5 with the surrounding ^{2}H-enriched cellular water. This in turn will lead to a ^{2}H-enrichment of the molecules in the TP and HP pool when photosynthetic carbohydrate supply is low.

(II) Sharkey & Weise (201**5**) postulate that at low photosynthetic carbohydrate supplies, the Calvin cycle is stabilized by means of the oxPPP replenishing the Calvin cycle intermediates with starch-derived pentose phosphates. Although starch is ^{2}H depleted, the first enzyme of the oxPPP (glucose-6-phosphate dehydrogenase) has been shown to strongly ^{2}H-enriche glucose-6-phosphate at C1 (Hermes et al., 1982). This will lead to ^{2}H-enrichment in glucose-6-phosphate and derivatives synthesized thereof when the oxPPP is upregulated (Wieloch *et al.* unpublished). Rearrangement of the photosynthetic carbohydrate metabolism in response to low photosynthetic carbohydrate supply might also induce a shift of stromal phosphoglucose isomerase towards equilibrium (Schleucher et al., 1999). This would result in the biosynthesis of ^{2}H-enriched transitory starch with downstream carbohydrates produced from the degradation of this starch also being ^{2}H-enriched (Wieloch *et al.* unpublished).

In essence it is a combination of different biochemical processes that act in concert and lead to plant organic compounds becomeing ^{2}H-enriched when photosynthetic carbohydrate supply to a plant's metabolism is low.

Interestingly, metabolic effects on ^{2}H-ε_{bio} values for α-cellulose were identical in both experiments. In contrast, effects on ^{2}H-ε_{bio} values for *n*-alkanes were much stronger when photosynthetic carbohydrate supply was reduced via the light reaction and plants were forced to utilize reserve carbohydrates as compared to photosynthetic carbohydrate supply being reduced via low pCO_2 and a limitation of the dark reaction of photosynthesis (Figs. 2 and 3). These observations are in line with the conceptual biochemical model for metabolic effects on the hydrogen isotope composition of plant organic compounds that we outlined above and can thus be used to validate our above considerations. Under low pCO_2 and under low light the biochemical source of H in the biosynthesis of carbohydrates is identical and comes from precursor molecules such as transitory or reserve starch that is converted to TP and HP that become ^{2}H-enriched under low photosynthetic carbohydrate supply (Fig. 1, 4). In contrast, the main source of H in lipids comes directly from NADPH (Fig. 1, 5). As the supplies of NADPH and the hydrogen isotope composition of NADPH from the light reaction of photosynthesis should not have been affected by our low pCO_2 treatment, the main H-source of lipids was consequently also unaffected by the CO_2 treatments. This explains why effects of low photosynthetic carbohydrate supplies triggered by low pCO_2 were comparatively small for ^{2}H-ε_{bio} of *n*-alkanes (Fig. 3c, e). In contrast, the metabolic effects on ^{2}H-ε_{bio} were stronger for *n*-alkanes when photosynthetic carbohydrate supplies were manipulated by low light and plants depended entirely on reserve metabolites for the biosynthesis of new organic compounds. The reason for this is that the biosynthesis of lipids from reserve carbohydrates via organic acids and acetyl-CoA requires additional NADPH-derived H (Figs. 4 and 5). In the absence of light this H cannot come from NADPH produced in the light reaction of photosynthesis but needs to be derived from NADPH that is generated heterotrophically, mainly in the oxPPP, and that has been shown to be ^{2}H-enriched compared to autotrophically reduced NADPH (Sessions *et al.*, 1999; Zhang *et al.*, 2009; Schmidt *et al.*, 2015). This suggests that in addition to the ^{2}H-enrichment of the biochemical precursor pools driven by the biochemical processes outlined above, the incorporation of additional and heterotrophically produced ^{2}H-

490 enriched NADPH, leads to larger metabolic effects on ^2H-ε_{bio} of lipids when
491 photosynthetic carbohydrate supplies are limited by the light reaction of
492 photosynthesis.
493
494 We found no effects of increasing $pCO_2 \geq 280$ ppm on ^2H-ε_{bio} in either compound class.
495 We suggest that this is because the size of the carbohydrate pools and/or the turnover
496 of the molecules in the pools was constant at $pCO_2 \geq 280$ ppm in our experiment. It has
497 been shown previously that the activity of RuBisCO is down-regulated with the
498 accumulation of soluble carbohydrates in the chloroplast or cytosol (Webber et al.,
499 1994). We thus suggest that at $pCO_2 \geq 280$ ppm the carbohydrate pool size was not
500 increasing enough in our experiment to significantly affect ^2H-ε_{bio} of α-cellulose or *n*-
501 alkanes. Similarly, we did not observe strong effects on ^2H-ε_{bio} above 5 μmol photons
502 m^{-2} s^{-1} for *n*-alkanes and above 115 μmol photons m^{-2} s^{-1} for α-cellulose. This indicates
503 that plants were already carbon autonomous with respect to the supply of fresh
504 carbohydrates from photosynthesis or that the main source of NADPH in the
505 biosynthesis of the compounds was coming from the light reaction of photosynthesis
506 above these light intensities rather than from the degradation of the reserves via the
507 oxPPP.
508
509 **Effects of photorespiration:** It has recently been shown that photorespiration can ^2H-
510 deplete the C-3 position of the 3-PGA (i.e. triose) (Ehlers et al., 2015). Photorespiration
511 occurs because RuBisCO can also catalyze the oxygenation of ribulose-1,5-
512 bisphosphate (RubP), a reaction that increases with declining CO_2 concentrations
513 (Bainbridge et al., 1995). This isotope effect of photorespiration should thus lead to ^2H-
514 ε_{bio} becoming progressively more negative at lower CO_2 concentrations, where rates of
515 photorespiration increase. An effect of photorespiration on ^2H-ε_{bio} of α-cellulose and *n*-
516 alkanes was, however, not detectable in our CO_2 experiment. As indicated in our model,
517 photorespiration seems to introduce ^2H-depleted H at the C-3 position of 3-PGA due to
518 the introduction of ^2H-depleted H atoms via the reaction ferredoxin
519 glutamine:oxoglutarate aminotransferase during the photorespiratory pathways
520 (Peterhansel et al., 2010) (Fig. 4). This ^2H-depleted C-3 position, which is transferred
521 to other positions without H isotope exchange during glucose and *n*-alkane biosynthesis
522 (Fig. 1 and 5), can affect up to 1 out of 7 and 9 out of 59 C-bound H atoms in a glucose

and in a C29-alkane molecule, respectively at high rates of photorespiration (Ehlers et al., 2015). It seems that these effects are too small to be detected in the δ^2H values of organic compounds or that the H isotopic changes associated with the cycling of the TP and HP pool and with the source of NADPH mask those of the photorespiration for α-cellulose and *n*-alkanes.

Effects of gluconeogenesis: Plants growing at low photosynthetic carbohydrate supply can utilize not only starch reserves as illustrated in our model but also lipid reserves to serve as C and energy source for the biosynthesis of compounds via gluconeogenesis. This is particularly relevant for plants growing from oil containing seeds. Luo & Sternberg (1992) have shown that plants growing from low photosynthetic supply from carbohydrate reserves (i.e. starch) have cellulose δ^2H values that are lower than plants growing from lipids. In plants with low photosynthetic carbohydrate supply that utilize lipids as their C and energy source, an important part of the precursor molecules for the production of new carbohydrates and lipids is acetyl-CoA, which is produced as a degradation product of the lipid β-oxidation that occurs via gluconeogenesis (Fig. 4). This important metabolic pathway results in a ^2H-enrichment of the acetyl-CoA pool by producing ^2H-depleted $FADH_2$ and NADH. Moreover, the action of enoyl CoA hydratase allows the exchange of C-bound H atoms with the surrounding ^2H-enriched foliar water. In the subsequent glyoxalate cycle, where two acetyl-CoA are used to produce succinate that will enter the TCA cycle and produce a new PEP, malate dehydrogenase will further ^2H-enrich the pool of succinate by producing ^2H-depleted NADH. As a result, carbohydrates produced by plants from lipid reserves are ^2H-enriched compared to carbohydrates that are produced from carbohydrate reserves (Agrawal & Canvin, 1971).

Post-photosynthetic ^2H-fractionation in plants with different photosynthetic pathways: Differences in δ^2H values of organic compounds have also been observed among plants that differ in their photosynthetic pathways (e.g. C_3, C_4 and Crassulacean Acid Metabolism (CAM)) (Sternberg *et al.*, 1984a; Chikaraishi *et al.*, 2004; Smith & Freeman, 2006; Feakins & Sessions, 2010a; Zhou *et al.*, 2011; Sachse *et al.*, 2012; Gamarra *et al.*, 2016). Specifically, carbohydrates and lipids in C_4 plants have generally been reported to be ^2H-enriched compared to those produced in C_3 plants. As suggested

by (Zhou *et al.*, 2016), the different anatomies of C_3 and C_4 plants influence ^2H-ε_{bio} via C-bound H exchanges with water of different anatomical compartments. For instance, intermediate compounds in C_4 plants exchange C-bound H with waters of the mesophyll cells that is ^2H-enriched compared to water in the bundle sheath cells, contributing to organic molecules that are ^2H-enriched compared to those produced by C_3 plants. This is in particular since the water in the mesophyll cells in C_4 plants should to be ^2H-enriched compared to the bulk leaf water values of C_3 plants (Gamarra *et al.*, 2016). Interestingly, our experimental treatments in the second experiment (where we included a C_4 plant *Zea mays*) show similar effects on ^2H-ε_{bio} of the C_4 plant than on the other investigated C_3 species (Fig S1). This suggests that metabolic effects of low photosynthetic carbohydrate supply on the ^2H-ε_{bio} of plant organic compounds are valid for plants with different photosynthetic pathways and that the δ^2H values of those plants equally record a low photosynthetic carbohydrate supply and/or a fast cycling of molecules in the TP and HP pools.

^2H-enrichment of organic compounds from CAM plants compared to organic compounds from C_3 plants that have been reported in the literature also agree with our conceptual model (Ziegler *et al.*, 1976; Feakins & Sessions, 2010b; Sachse *et al.*, 2012). During the day, when CAM plants release CO_2 via NAD(P)-malic enzyme (ME) from the malic acid and perform photosynthesis by using this CO_2, the resulting C_3 compounds are used to produce starch via the same biosynthetic pathway, i.e. the gluconeogenesis, that is used after lipid degradation in regular C_3 plants. This mechanism leads to an intense cycling of malic acid and pyruvate and consequently a ^2H-enrichment of the involved molecules that ultimately lead to the TP and organic acid pool in the cytosol (Fig. 4). Interestingly, Sternberg *et al.* (1984a) observed that the cellulose produced by CAM plants is ^2H-enriched compared to lipids produced by the same plants. This is in agreement with our model and supports the idea that the cycling of organic precursors pools (such as pyruvate and malic acid or hexose and triose) and the extraction of light H via the reduction of $NAD(P)^+$ is an important driver for the ^2H-ε_{bio} of carbohydrates. This cycling seems to be a less important driver of the ^2H-ε_{bio} in lipids biosynthesis as their main source of H comes from the NADPH produced in the chloroplast (Fig. 4).

^{2}H as a proxy for the C metabolism of plants: The motivation of our study was to identify how and where ^{2}H-fractionation occurs during photosynthetic and post-photosynthetic biosynthetic processes in plants. With this, we want to provide a mechanistic basis for understanding differences in ^{2}H-ε_{bio} for different compound classes in plants and, most importantly, to set the mechanistic ground for the application of plant δ^2H values as proxy for a plant's C metabolism. Our experiments show substantial differences in the δ^2H values of carbohydrates and lipids that can largely be explained by the higher proportion of NADPH-derived and ^{2}H-depleted H in lipids compared to carbohydrates. We show strong effects of low photosynthetic carbohydrate supply on the biosynthetic hydrogen isotope fractionation for both, carbohydrates and lipids. For carbohydrates, the metabolic effects on ^{2}H-ε_{bio} were independent of the causes of low carbohydrate supply to the plant and were surprisingly robust across species and compound classes. For lipids, effects were stronger when plants were forced to utilize reserve carbohydrates in their metabolism and to generate NADPH for the biosynthesis of lipids via heterotrophic pathways.

Being able to interpret metabolic variability in the δ^2H values of plant organic compounds that is beyond hydrological forcing will help to resolve previously explained variability in the δ^2H values of plant organic compounds in sediment records or in tree rings when these are applied as a (paleo-)hydrological signals. Most importantly, however, understanding the metabolic effects that shape the δ^2H values of plant organic compounds will open new opportunities to utilize plant δ^2H values to address the carbon metabolism of plants and ecosystems. While we show here, that photosynthetic carbohydrate supply has a key effect on the δ^2H values of plant organic compounds, previous studies have already employed δ^2H values of *n*-alkanes or cellulose to indicate the carbon autonomy of plant tissues, plant organs or entire plants (Gamarra & Kahmen, 2015; Newberry *et al.*, 2015; Kimak *et al.*, 2015; Gebauer *et al.*, 2016). With our conceptual biochemical model, we can now explain why organic compounds in non-C autonomous tissue with low photosynthetic carbohydrate supplies become ^{2}H-enriched. By comparing effects on carbohydrates and lipids, we can even differentiate if limitations of the light or dark reaction cause plant tissue to be carbon limited.

The model we present here will be particularly instrumental to interpret non-hydrological signals in δ^2H values of plant organic compounds when these are analysed in combination with $\delta^{18}O$ values. This is, because $\delta^{18}O$ values are driven only by hydrological drivers (source water $\delta^{18}O$ and leaf water $\delta^{18}O$ (Roden et al., 2000; Kahmen et al., 2011) and the combined analysis of δ^2H and $\delta^{18}O$ values should thus allow to disentangle hydrological and metabolic effects, e.g. in tree ring or sediment records. Such an application of δ^2H values in plant organic compounds could allow for the first time to assess long-term metabolic responses of plants and ecosystems to global environmental change and to address important feedbacks between the coupled climate carbon cycle. While a quantitative link between a plants carbon metabolism and variability in the δ^2H values will have to be established in future studies, the experiments that we present here, and the conceptual biochemical model that resulted from these experiments, set the foundation for establishing plant δ^2H values as a fundamentally important new metabolic proxy that will be relevant for a broad range of disciplines, including plant physiology, plant breeding, ecology, biogeochemistry, paleoecology and earth system sciences.

Acknowledgement

M.A.C. and A.K. were both funded by the ERC starting grant COSIWAX (ERC-2011-StG Grant Agreement No. 279518) to A.K. We thank Rolf Siegwolf (PSI) and Adam Kimak (Bern) for their help with the cellulose extractions and measurements.

References

Agrawal PK, Canvin DT. **1971**. The pentose phosphate pathway in relation to fat synthesis in the developing castor oil seed. *Plant Physiology* **47**: 672–675.

Allen DK, Bates PD, Tjellström H. **2015**. Tracking the metabolic pulse of plant lipid production with isotopic labeling and flux analyses: Past, present and future. *Progress in Lipid Research* **58**: 97–120.

Augusti A, Betson TR, Schleucher J. **2006**. Hydrogen exchange during cellulose synthesis distinguishes climatic and biochemical isotope fractionations in tree rings.

New Phytologist **172**: 490–499.

Baillif V, Robins RJ, Le Feunteun S, Lesot P, Billault I. **2009**. Investigation of fatty acid elongation and desaturation steps in *Fusarium lateritium* by quantitative two-dimensional deuterium NMR spectroscopy in chiral oriented media. *Journal of Biological Chemistry* **284**: 10783–10792.

Bainbridge G, Madgwick P, Parmar S, Mitchell R, Paul M, Pitts J, Keys AJ, Parry MAJ. **1995**. Engineering Rubisco to change its catalytic properties. *Journal of Experimental Botany* **46**: 1269–1276.

Barbour MM. **2007**. Stable oxygen isotope composition of plant tissue: a review. *Functional Plant Biology* **34**: 83–94.

Blanchard JS, Cleland WW. **1980**. Use of isotope effects to deduce the chemical mechanism of fumarase. *Biochemistry* **19**: 4506–4513.

Buchanan BB, Gruissem W, Vickers K, Jones RL. **2015**. *Biochemistry and molecular biology of plants*. New York: Wiley and sons.

Burgoyne TW, Hayes JM. **1998**. Quantitative production of H_2 by pyrolysis of gas chromatographic effluents. *Analytical Chemistry* **70**: 5136–5141.

Cernusak LA, Barbour MM, Arndt SK, Cheesman AW, English NB, Feild TS, Helliker BR, Holloway Phillips MM, Holtum JAM, Kahmen A, *et al.* 2016. Stable isotopes in leaf water of terrestrial plants. *Plant, Cell and Environment* **39**: 1087–1102.

Cheesbrough TM, Kolattukudy PE. **1984**. Alkane biosynthesis by decarbonylation of aldehydes catalyzed by a particulate preparation from *Pisum sativum*. *Proceedings of the National Academy of Sciences* **81**: 6613–6617.

Chikaraishi Y, Naraoka H. **2003**. Compound-specific $\delta D–\delta^{13}C$ analyses of *n*-alkanes extracted from terrestrial and aquatic plants. *Phytochemistry* **63**: 361–371.

Chikaraishi Y, Naraoka H, Poulson SR. **2004**. C and hydrogen isotopic fractionation during lipid biosynthesis in a higher plant (*Cryptomeria japonica*). *Phytochemistry* **65**: 323–330.

Dawson KS, Osburn MR, Sessions AL, Orphan VJ. **2015**. Metabolic associations with archaea drive shifts in hydrogen isotope fractionation in sulfate-reducing bacterial lipids in cocultures and methane seeps. *Geobiology* **13**: 462–477.

Dawson TE, Mambelli S, Plamboeck AH, Templer PH, Tu KP. **2002**. Stable isotopes in plant ecology. *Annual Review of Ecology and Systematics* **33**: 507–559.

Dorrer HD, Fedtke C, Trebst A. **1966**. Intramolekulare Wasserstoffverschiebung in der Hexosephosphatisomerase Reaktion bei der photosynthetischen Stärkebildung in Chlorella. *Chlorella. Z. Naturforschg*: 557–562.

Drake BG, Gonzalez-Meler MA, Long SP. **1997**. More efficient plants: a consequence of rising atmospheric CO_2. *Annual review of plant physiology and plant*

molecular biology **48**: 609–639.

Ehlers I, Augusti A, Betson TR, Nilsson MB, Marshall JD, Schleucher J. **2015**. Detecting long-term metabolic shifts using isotopomers: CO_2-driven suppression of photorespiration in C3 plants over the 20th century. *Proceedings of the National Academy of Sciences*: 201504493–10.

Epstein S, Yapp CJ, Hall JH. **1976**. The determination of the D/H ratio of non-exchangeable hydrogen in cellulose extracted from aquatic and land plants. *Earth and Planetary Science Letters* **30**: 241–251.

Estep MF, Hoering TC. **1980**. Biogeochemistry of the stable hydrogen isotopes. *Geochimica et Cosmochimica Acta* **44**: 1197–1206.

Feakins SJ, Sessions AL. **2010a**. Controls on the D/H ratios of plant leaf waxes in an arid ecosystem. *Geochimica et Cosmochimica Acta* **74**: 2128–2141.

Feakins SJ, Sessions AL. **2010b**. Crassulacean acid metabolism influences D/H ratio of leaf wax in succulent plants. *Organic Geochemistry* **41**: 1269–1276.

Fiedler F, Müllhofer G, Trebst A, Rose IA. **1967**. Mechanism of Ribulose-Diphosphate Carboxydismutase Reaction. *European Journal of Biochemistry* **1**: 395–399.

Filot MS, Leuenberger M, Pazdur A, Boettger T. **2006**. Rapid online equilibration method to determine the D/H ratios of non-exchangeable hydrogen in cellulose. *Rapid Communications in Mass Spectrometry* **20**: 3337–3344.

Gamarra B, Kahmen A. **2015**. Concentrations and δ^2H values of cuticular n-alkanes vary significantly among plant organs, species and habitats in grasses from an alpine and a temperate European grassland. *Oecologia* **178**: 981–998.

Gamarra B, Sachse D, Kahmen A. **2016**. Effects of leaf water evaporative 2H-enrichment and biosynthetic fractionation on leaf wax n-alkane δ2H values in C3 and C4 grasses. *Plant, Cell and Environment* **11**: 2390 – 2403.

Gaudinski JB, Dawson TE, Quideau S, Schuur EAG, Roden JS, Trumbore SE, Sandquist DR, Oh S-W, Wasylishen RE. **2005**. Comparative analysis of cellulose preparation techniques for use with ^{13}C, ^{14}C, and ^{18}O isotopic measurements. *Analytical Chemistry* **77**: 7212–7224.

Gebauer G, Preiss K, Gebauer AC. **2016**. Partial mycoheterotrophy is more widespread among orchids than previously assumed. *New Phytologist* **211**: 11–15.

Gehre M, Geilmann H, Richter J, Werner RA, Brand WA. **2004**. Continuous flow ^{2}H/^{1}H and ^{18}O/^{16}O analysis of water samples with dual inlet precision. *Rapid Communications in Mass Spectrometry* **18**: 2650–2660.

Gerhart LM, Ward JK. **2010**. Plant responses to low [CO2] of the past. *New Phytologist* **188**: 674–695.

Hall DR, Leonard GA, Reed CD, Watt CI, Berry A, Hunter WN. **1999**. The

crystal structure of *Escherichia coli* class II fructose-1,6-bisphosphate aldolase in complex with phosphoglycolohydroxamate reveals details of mechanism and specificity. *Journal of Molecular Biology* **287**: 383–394.

Heldt HW, Piechulla B, Heldt F. **2005**. *Plant Biochemistry*. Elsevier.

Hermes JD, Roeske CA, O'Leary MH, Cleland WW. **1982**. Use of multiple isotope effects to determine enzyme mechanisms and intrinsic isotope effects - malic enzyme and glucose-6-phosphate-dehydrogenase. *Biochemistry* **21**: 5106–5114.

Hill SA, Waterhouse JS, Field EM, Switsur VR, Rees TA. **1995**. Rapid recycling of triose phosphates in oak stem tissue. *Plant, Cell and Environment* **18**: 931–936.

Hou J, D'Andrea WJ, Huang Y. **2008**. Can sedimentary leaf waxes record D/H ratios of continental precipitation? Field, model, and experimental assessments. *Geochimica et Cosmochimica Acta* **72**: 3503–3517.

Igamberdiev AU, Gardeström P. **2003**. Regulation of NAD- and NADP-dependent isocitrate dehydrogenases by reduction levels of pyridine nucleotides in mitochondria and cytosol of pea leaves. *Biochimica et Biophysica Acta (BBA) - Bioenergetics* **1606**: 117–125.

Kahmen A, Hoffmann B, Schefuß E, Arndt SK, Cernusak LA, West JB, Sachse D. **2013a**. Leaf water deuterium enrichment shapes leaf wax n-alkane δD values of angiosperm plants II: Observational evidence and global implications. *Geochimica et Cosmochimica Acta* **111**: 50–63.

Kahmen A, Sachse D, Arndt SK, Tu KP, Farrington H, Vitousek PM, Dawson TE. **2011**. Cellulose $\delta^{18}O$ is an index of leaf-to-air vapor pressure difference (VPD) in tropical plants. *Proceedings of the National Academy of Sciences of the United States of America* **108**: 1981–1986.

Kahmen A, Schefuß E, Sachse D. **2013b**. Leaf water deuterium enrichment shapes leaf wax n-alkane δD values of angiosperm plants I: Experimental evidence and mechanistic insights. *Geochimica et Cosmochimica Acta* **111**: 39–49.

Kazuki S, Akihiko K, Shigenobu O, Yousuke S, Tamio Y. **1980**. Incorporation of hydrogen atoms from deuterated water and stereospecifically deuterium-labeled nicotinamide nucleotides into fatty acids with the Escherichia coli fatty acid synthetase system. *Biochimica et Biophysica Acta (BBA) - Lipids and Lipid Metabolism* **618**: 202–213.

Kestler DP, Mayne BC, Ray TB, Goldstein LD. **1975**. Biochemical components of the photosynthetic CO 2 compensation point of higher plants. *Biochemical and biophysical research communications* **66**: 1439–1446.

Kimak A, Kern Z, Leuenberger M. **2015**. Qualitative distinction of autotrophic and heterotrophic processes at the leaf level by means of triple stable isotope (C–O–H) patterns. *Frontiers in Plant Science* **6**: 490.

Knowles JR, Albery WJ. **1977**. Perfection in enzyme catalysis: the energetics of triosephosphate isomerase. *Accounts of Chemical Research* **10**: 105–111.

Krenzer EG, Moss DN. **1969**. C Dioxide Compensation in Grasses. *Crop Science* **9**: 619–621.

Liu Z, Huang Y. **2008**. Hydrogen isotopic compositions of plant leaf lipids are unaffected by a twofold pCO2 change in growth chambers. *Organic Geochemistry* **39**: 478–482.

Luo Y-H, Sternberg LDSLO. **1991**. Deuterium heterogeneity in starch and cellulose nitrate of cam and C3 plants. *Phytochemistry* **30**: 1095–1098.

Luo Y-H, Sternberg LDSLO. **1992**. Hydrogen and oxygen isotopic fractionation during heterotrophic cellulose synthesis. *Journal of Experimental Botany* **43**: 47–50.

Luo Y-H, Sternberg LDSLO, Suda S, Kumazawa S, Mitsui A. **1991**. Extremely low D/H ratios of photoproduced hydrogen by cyanobacteria. *Plant and cell physiology* **32**: 897–900.

Magill CR, Ashley GM, Freeman KH. **2013**. Water, plants, and early human habitats in eastern Africa. *Proceedings of the National Academy of Sciences of the United States of America* **110**: 1175–1180.

Maister SG, Pett CP, Albery WJ, Knowles JR. **1976**. Energetics of triosephosphate isomerase: the appearance of solvent tritium in substrate dihydroxyacetone phosphate and in product. *Biochemistry* **15**: 5607–5612.

Møller IM, Rasmusson AG. **1998**. The role of NADP in the mitochondrial matrix. *Trends in Plant Science* **3**: 21–27.

Newberry SL, Kahmen A, Dennis P, Grant A. **2015**. *n*-Alkane biosynthetic hydrogen isotope fractionation is not constant throughout the growing season in the riparian tree *Salix viminalis*. *Geochimica et Cosmochimica Acta* **165**: 75–85.

Pedentchouk N, Sumner W, Tipple B, Pagani M. **2008**. δ13C and δD compositions of n-alkanes from modern angiosperms and conifers: An experimental set up in central Washington State, USA. *Organic Geochemistry* **39**: 1066–1071.

Peterhansel C, Horst I, Niessen M, Blume C, Kebeish R, Kürkcüoglu S, Kreuzaler F. **2010**. Photorespiration. *The Arabidopsis Book* **8**: e0130.

Peters KE, Walters CC, Moldowan JM. **2005**. *The Biomarker Guide: Biomarkers and isotopes in the environment and human history*. Cambridge University Press.

Rach O, Brauer A, Wilkes H, Sachse D. **2014**. Delayed hydrological response to Greenland cooling at the onset of the Younger Dryas in western Europe. *Nature Geoscience* **7**: 1–4.

Rambeck WA, Bassham JA. **1973**. Tritium incorporation and retention in photosynthesizing algae. *Biochimica et Biophysica Acta (BBA) - General Subjects* **304**: 725–735.

Rieder SV, Rose IA. **1959**. The mechanism of the triosephosphate isomerase reaction. *Journal of Biological Chemistry* **234**: 1007–1010.

Roden JS, Lin G, Ehleringer JR. **2000**. A mechanistic model for interpretation of hydrogen and oxygen isotope ratios in tree-ring cellulose. *Geochimica et Cosmochimica Acta* **64**: 21–35.

Rose IA, Rieder SV. **1958**. Studies on the mechanism on the aldolase reaction; isotope exchange reactions of muscle and yeast aldolase. *Journal of Biological Chemistry* **231**: 315–329.

Sachse D, Billault I, Bowen GJ, Chikaraishi Y, Dawson TE, Feakins SJ, Freeman KH, Magill CR, McInerney FA, van der Meer MTJ, *et al.* 2012. Molecular paleohydrology: Interpreting the hydrogen-isotopic composition of lipid biomarkers from photosynthesizing organisms. *Annual Review of Earth and Planetary Sciences* **40**: 221–249.

Sachse D, Radke J, Gleixner G. **2004**. Hydrogen isotope ratios of recent lacustrine sedimentary n-alkanes record modern climate variability. *Geochimica et Cosmochimica Acta* **68**: 4877–4889.

Sachse D, Radke J, Gleixner G. **2006**. δD values of individual *n*-alkanes from terrestrial plants along a climatic gradient – Implications for the sedimentary biomarker record. *Organic Geochemistry* **37**: 469–483.

Sauer PE, Schimmelmann A, Sessions AL, Topalov K. **2009**. Simplified batch equilibration for D/H determination of non-exchangeable hydrogen in solid organic material. *Rapid Communications in Mass Spectrometry* **23**: 949–956.

Schimmelmann A. **1991**. Determination of the Concentration and Stable Isotopic Composition of Nonexchangeable Hydrogen in Organic-Matter. *Analytical Chemistry* **63**: 2456–2459.

Schirmer A, Rude MA, Li X, Popova E, del Cardayre SB. **2010**. Microbial biosynthesis of akanes. *Science* **329**: 559–562.

Schleucher J, Vanderveer P, Markley JL, Sharkey TD. **1999**. Intramolecular deuterium distributions reveal disequilibrium of chloroplast phosphoglucose isomerase. *Plant, Cell and Environment* **22**: 525–533.

Schmidt H-L, Robins RJ, Werner RA. **2015**. Multi-factorial *in vivo* stable isotope fractionation: causes, correlations, consequences and applications. *Isotopes in environmental and health studies* **51**: 155–199.

Schmidt H-L, Werner RA, Eisenreich W. **2003**. Systematics of ^{2}H patterns in natural compounds and its importance for the elucidation of biosynthetic pathways. *Phytochemistry Reviews* **2**: 61–85.

Sessions AL. **2006**. Isotope-ratio detection for gas chromatography. *Journal of Separation Science* **29**: 1946–1961.

Sessions AL, Burgoyne TW, Schimmelmann A, Hayes JM. **1999**. Fractionation of hydrogen isotopes in lipid biosynthesis. *Organic Geochemistry* **30**: 1193–1200.

Sharkey TD, Weise SE. **2016**. The glucose 6-phosphate shunt around the Calvin–

847 Benson cycle. *Journal of Experimental Botany* **67**: 4067–4077.

848 **Silverman RB**. **2002**. *The organic chemistry of enzyme-catalyzed reactions*. San
849 Diego : Academic Press.

850 **Smith BN, Epstein S**. **1970**. Biogeochemistry of the stable isotopes of hydrogen and
851 C in salt marsh biota. *Plant Physiology* **46**: 738–742.

852 **Smith FA, Freeman KH**. **2006**. Influence of physiology and climate on δD of leaf
853 wax *n*-alkanes from C_3 and C_4 grasses. *Geochimica et Cosmochimica Acta* **70**: 1172–
854 1187.

855 **Sternberg LDSL, Anderson WT, Morrison K**. **2003**. Separating soil and leaf water
856 18O isotopic signals in plant stem cellulose. *Geochimica et Cosmochimica Acta* **67**:
857 2561–2566.

858 **Sternberg LDSLO, DeNiro MJ, Ajie H**. **1984a**. Stable hydrogen isotope ratios of
859 saponifiable lipids and cellulose nitrate from CAM, C_3 and C_4 plants. *Phytochemistry*
860 **23**: 2475–2477.

861 **Sternberg LDSLO, DeNiro MJ, Ting IP**. **1984b**. C, hydrogen, and oxygen isotope
862 ratios of cellulose from plants having intermediary photosynthetic modes. *Plant*
863 *Physiology* **74**: 104–107.

864 **Stocker TF, Dahe Q, Plattner G-K**. **2013**. Climate Change 2013: The Physical
865 Science Basis. *Working Group I Contribution to the Fifth Assessment Report of the*
866 *Intergovernmental Panel on Climate Change. Summary for Policymakers (IPCC,*
867 *2013)*.

868 **Tripati AK, Roberts CD, Eagle RA**. **2009**. Coupling of CO_2 and ice sheet stability
869 over major climate transitions of the last 20 Million years. *Science* **326**: 1394–1397.

870 **Voet D, Voet JG**. **2011**. *Biochemistry, 4th Edition*. New York: John Wiley & Sons.

871 **Wang Y, Sessions AL, Nielsen RJ, Goddard WA III**. **2009**. Equilibrium 2 H/1 H
872 fractionations in organic molecules. II: Linear alkanes, alkenes, ketones, carboxylic
873 acids, esters, alcohols and ethers. *… et Cosmochimica Acta* **73**: 7076–7086.

874 **Webber AN, Nie G-Y, Long SP**. **1994**. Acclimation of photosynthetic proteins to
875 rising atmospheric CO2. *Photosynthesis Research* **39**: 413–425.

876 **West AG, Patrickson SJ, Ehleringer JR**. **2006**. Water extraction times for plant and
877 soil materials used in stable isotope analysis. *Rapid Communications in Mass*
878 *Spectrometry* **20**: 1317–1321.

879 **White D, Drummond JT, Fuqua C**. **2012**. *The Physiology and Biochemistry of*
880 *Prokaryotes*. Oxford University Press, USA.

881 **White JWC**. **1989**. Stable Hydrogen Isotope Ratios in Plants: A Review of Current
882 Theory and Some Potential Applications. Ecological Studies. Stable isotopes in
883 ecological research. New York, NY: Springer New York, 142–162.

884 **Wieloch T, Yu J, Ehlers I, Grabner M, Marshall JD, Schleucher J**. Metabolic
885 regulation can be a major determinant of plant glucose D variability (*in preparation*).

886 **Yakir D**. **1992**. Variations in the natural abundance of oxygen-18 and deuterium in
887 plant carbohydrates. *Plant, Cell and Environment* **15**: 1005–1020.

888 **Yakir D, DeNiro MJ**. **1990**. Oxygen and hydrogen isotope fractionation during
889 cellulose metabolism in *Lemna gibba* L. *Plant Physiology* **93**: 325–332.

890 **Zhang X, Gillespie AL, Sessions AL**. **2009**. Large D/H variations in bacterial lipids
891 reflect central metabolic pathways. *Proceedings of the National Academy of Sciences*
892 **106**: 12580–12586.

893 **Zhou Y, Grice K, Chikaraishi Y, Stuart-Williams H, Farquhar GD, Ohkouchi N**.
894 **2011**. Phytochemistry. *Phytochemistry* **72**: 207–213.

895 **Zhou Y, Grice K, Stuart-Williams H, Hocart CH, Gessler A, Farquhar GD**.
896 **2016**. Hydrogen isotopic differences between C3 and C4 land plant lipids:
897 consequences of compartmentation in C4 photosynthetic chemistry and C3
898 photorespiration. *Plant, Cell and Environment*.

899 **Ziegler H**. **1989**. Hydrogen Isotope fractionation in plant tissues. Ecological Studies.
900 Stable isotopes in ecological research. New York, NY: Springer New York, 105–123.

901 **Ziegler H, Osmond CB, Stichler W, Trimborn P**. **1976**. Hydrogen isotope
902 discrimination in higher-plants - Correlations with photosynthetic pathway and
903 environment. *Planta* **128**: 85–92.

904

Figures

Fig. 1. Different biochemical origins of H atoms in the biosynthesis of plant organic compounds. We illustrate the different origins for the biosynthesis of glucose but similar processes occur in all biochemical pathways. Black H are coming from the precursor ribulose-1,5-bisphosphate, blue H are coming from the surrounding water, green H are originating from NADPH. * means that half of H atoms at this position are coming from the cellular water, the rest are from the precursor molecule. Waves represent H atoms that partially exchange with surrounding water through H addition to sp^2 hybridized-C atoms (i.e. C=C) or by (partial) exchange of C-bound H atoms in CH_2-groups adjacent to CO-groups. Key enzymes and molecules are indicated by their following abbreviations: 3-PGA, 3-phosphoglycerate; ALD, aldolase; DHAP, dihydroxyacetone phosphate; FBPase, fructose 1,6-bisphosphatase; FBP, fructose 1,6-bisphosphate; F6P, fructose 6-phosphate; GAP, glyceraldehyde 3-phosphate; GAPDH, glyceraldehyde 3-phosphate dehydrogenase; $NADP^+$, nicotinamide adenine dinucleotide phosphate; PGI, phosphoglucose isomerase; PGK, phosphoglycerate kinase; PRP, photorespiratory pathway; RuBisCO, ribulose-1,5-bisphosphate carboxylase/oxygenase; TPI, triosephosphate isomerase. The red H represent the ^{2}H-depleted atoms that can come from the 3-phosphoglycerate produced upon the photosynthetic C oxidation during photorespiration (Rieder & Rose, 1959; Knowles & Albery, 1977; Schleucher *et al.*, 1999; Augusti *et al.*, 2006; Buchanan *et al.*, 2015).

Fig. 2. Leaf water, α-cellulose, *n*-alkane δ^2H values and Δ^2H-ε_{bio} for α-cellulose and *n*-alkanes under different pCO_2 averaged across all six species. The magnitude of ^{2}H-ε_{bio} can differ largely across different species. To allow the comparison of treatment effects on ^{2}H-ε_{bio} across all six species we standardized the ^{2}H-ε_{bio} response of a species to the pCO2 treatment around its overall mean ^{2}H-ε_{bio} in the experiment (i.e. Δ^2H-ε_{bio}). Each point corresponds to the averaged values 6 different species (n=6) grown in 3 replicates from seeds under the different pCO_2. The ^{2}H-ε_{bio} curves for individual species are available of Fig. S1.

Fig. 3. Leaf water, α-cellulose, *n*-alkane δ^2H values and the corresponding relative ^{2}H-ε_{bio} for α-cellulose and *n*-alkanes under different light intensities (photosynthetic active radiation, PhAR) averaged across all six species. The magnitude of ^{2}H-ε_{bio} can differ largely across different species. To allow the comparison of treatment effects on ^{2}H-ε_{bio} across all six species we standardized the ^{2}H-ε_{bio} response of a species to the light treatment around its overall mean ^{2}H-ε_{bio} in the experiment (i.e. Δ^2H ε_{bio}). Each point corresponds to the averaged values 6 different species (n=6) grown in 3 replicates from the tuber or roots under the different light intensity. The ^{2}H-ε_{bio} curves for individual species are available of Fig. S2.

Fig. 4. Schematic view of H flow during processes leading to *n*-alkanes and α-cellulose ^{2}H-ε_{bio}. The key enzymes and pathways responsible for H flow are indicated by their following abbreviations and are based on known biochemical pathways (Rose & Rieder, 1958; Rieder & Rose, 1959; Knowles & Albery, 1977; Cheesbrough & Kolattukudy, 1984; Schleucher et al., 1999; Heldt et al., 2005; Augusti et al., 2006; Zhang et al., 2009; Schirmer et al., 2010; Voet & Voet, 2011; Buchanan et al., 2015; Ehlers et al., 2015). The Roman numerals indicate the two main post-photosynthetic biochemical processes that we suggest to be responsible for the general ^{2}H-enrichment of plant metabolites under low photosynthetic carbohydrate supply: 2-OGDH, 2-oxoglutarate dehydrogenase; 6PGD, 6-phosphogluconate dehydrogenase; ACP, acyl-carrier-protein; ALD, aldolase; ENO, enolase; Fd-GOGAT, ferredoxin glutamine:oxoglutarate aminotransferase; FNR, ferredoxin-$NADP^+$ reductase; G6PDH, glucose-6-phosphate dehydrogenase; GAP, glyceraldehyde 3-phosphate; GAPDH, glyceraldehyde 3-phosphate dehydrogenase; IDH, isocitrate dehydrogenase; KA, ketoacyl; ME, malic enzyme; NADP, nicotinamide adenine dinucleotide; NADPH, nicotinamide adenine dinucleotide phosphate; ME, malate dehydrogenase; PDH, pyruvate dehydrogenase; PEP, phosphoenolpyruvate; PGI, phosphoglucose isomerase; PK, pyruvate kinase; oxPPP, oxidative pentose phosphate pathway; TPI, triosephosphate isomerase; TE, *trans*-enoyl; TPT, triose phosphate translocator; R, reductase; RuBisCO, ribulose-1,5-bisphosphate carboxylase/oxygenase. Succinate dehydrogenase also produced $FADH_2$ in the TCA cycle, but is not represented on the scheme.

Fig. 5. Simplified view of the biochemical origins of H atoms in *n*-alkane biosynthesis. Black H represent H atoms from the precursor acetyl-CoA. Green H originate from NADPH reduced by the light reaction of photosynthesis in the chloroplast and or by oxPPP and other reactions in the endoplasmic reticulum. Blue H are from H atoms in equilibrium with surrounding water. The fatty acids are generally elongated

963 until 16 or 18 Cs long in the chloroplast and until 32 Cs long in the endoplasmic reticulum; this might
964 also imply different H sourcing (Cheesbrough & Kolattukudy, 1984; Zhang et al., 2009; Schirmer et al.,
965 2010; Buchanan et al., 2015). The red H represent the ^{2}H-depleted atoms that can come from the 3-
966 phosphoglycerate produced upon the photosynthetic C oxidation. In a C29-alkane, of 60 H atoms, 28
967 comes from NADPH, 14 from water, 17 from manolyl-ACP (which ultimately derives from acetyl-CoA
968 and pyruvate).
969

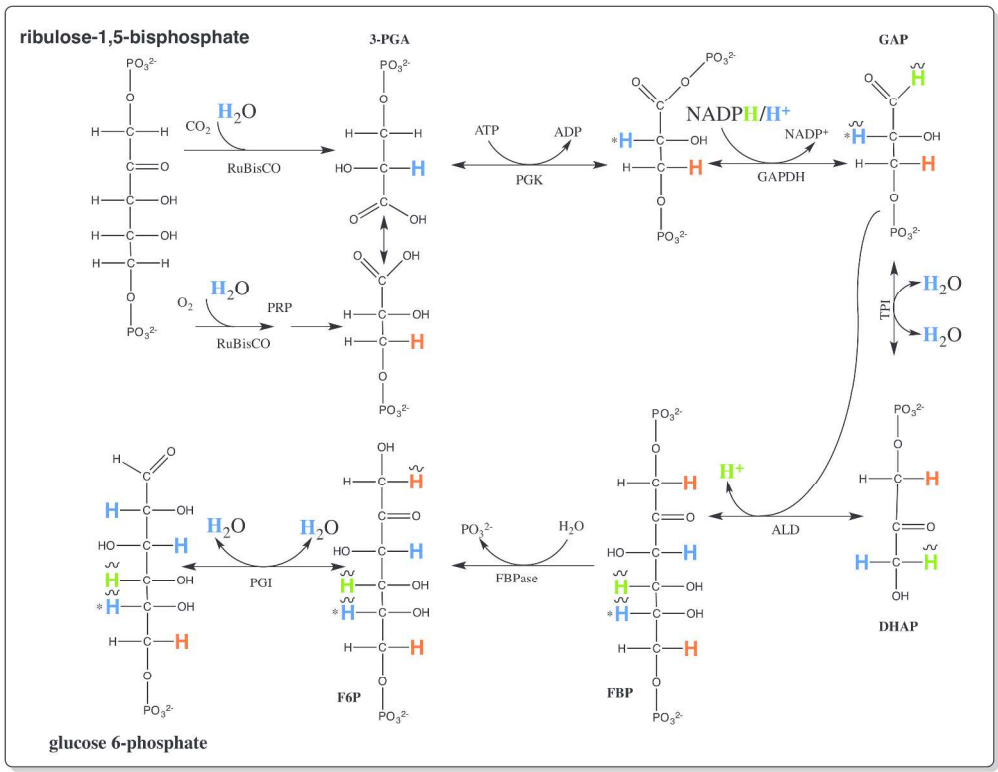

Fig. 1. Different biochemical origins of H atoms in the biosynthesis of plant organic compounds. We illustrate the different origins for the biosynthesis of glucose but similar processes occur in all biochemical pathways. Black H are coming from the precursor ribulose-1,5-bisphosphate, blue H are coming from the surrounding water, green H are originating from NADPH. * means that half of H atoms at this position are coming from the cellular water, the rest are from the precursor molecule. Waves represent H atoms that partially exchange with surrounding water through H addition to sp2 hybridized-C atoms (i.e. C=C) or by (partial) exchange of C-bound H atoms in CH_2-groups adjacent to CO-groups. Key enzymes and molecules are indicated by their following abbreviations: 3-PGA, 3-phosphoglycerate; ALD, aldolase; DHAP, dihydroxyacetone phosphate; FBPase, fructose 1,6-bisphosphatase; FBP, fructose 1,6-bisphosphate; F6P, fructose 6-phosphate; GAP, glyceraldehyde 3-phosphate; GAPDH, glyceraldehyde 3-phosphate dehydrogenase; $NADP^+$, nicotinamide adenine dinucleotide phosphate; PGI, phosphoglucose isomerase; PGK, phosphoglycerate kinase; PRP, photorespiratory pathway; RuBisCO, ribulose-1,5-bisphosphate carboxylase/oxygenase; TPI, triosephosphate isomerase. The red H represent the ^{2}H-depleted atoms that can come from the 3-phosphoglycerate produced upon the photosynthetic C oxidation during photorespiration (Rieder & Rose, 1959; Knowles & Albery, 1977; Schleucher et al., 1999; Augusti et al., 2006; Buchanan et al., 2015)

305x235mm (300 x 300 DPI)

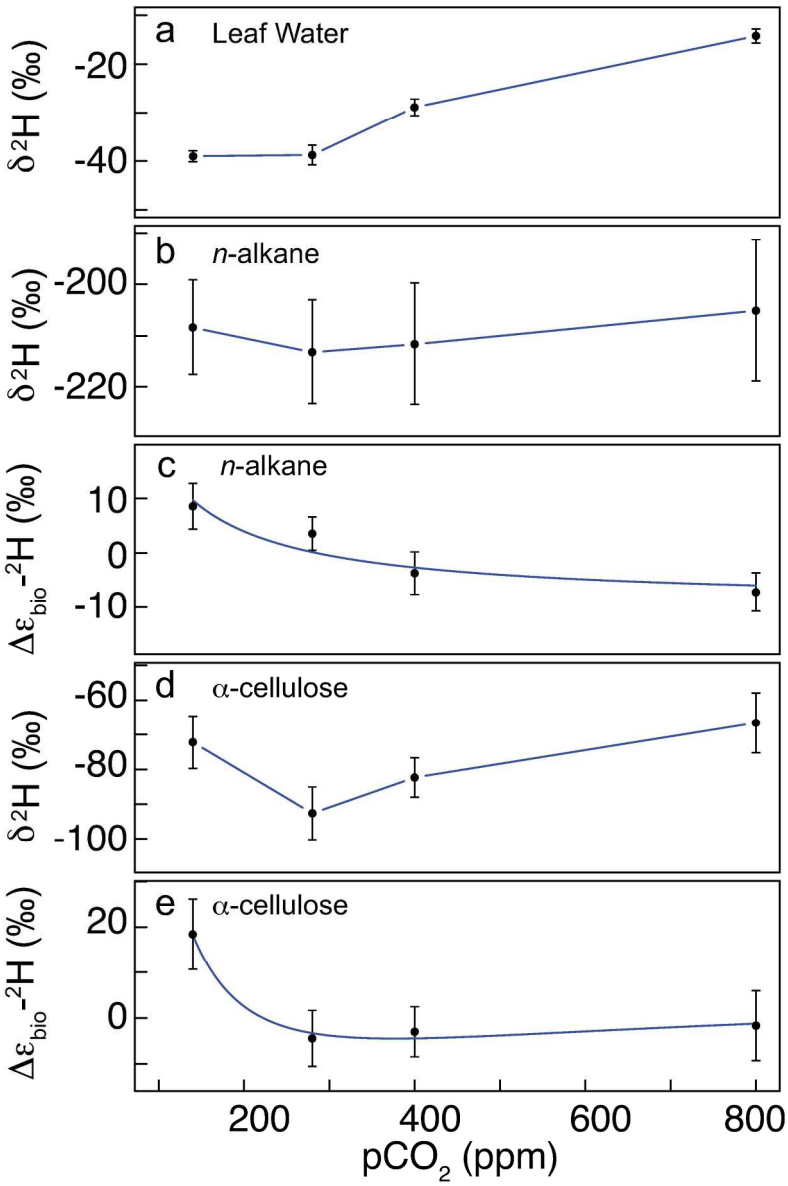

Fig. 2. Leaf water, α-cellulose, *n*-alkane δ^2H values and Δ^2H-ε_{bio} for α-cellulose and *n*-alkanes under different pCO_2 averaged across all six species. The magnitude of ^2H-ε_{bio} can differ largely across different species. To allow the comparison of treatment effects on ^2H-ε_{bio} across all six species we standardized the ^2H-ε_{bio} response of a species to the pCO_2 treatment around its overall mean ^2H-ε_{bio} in the experiment (i.e. Δ^2H-ε_{bio}). Each point corresponds to the averaged values 6 different species (n=6) grown in 3 replicates from seeds under the different pCO_2. The ^2H-ε_{bio} curves for individual species are available of Fig. S1.

180x262mm (300 x 300 DPI)

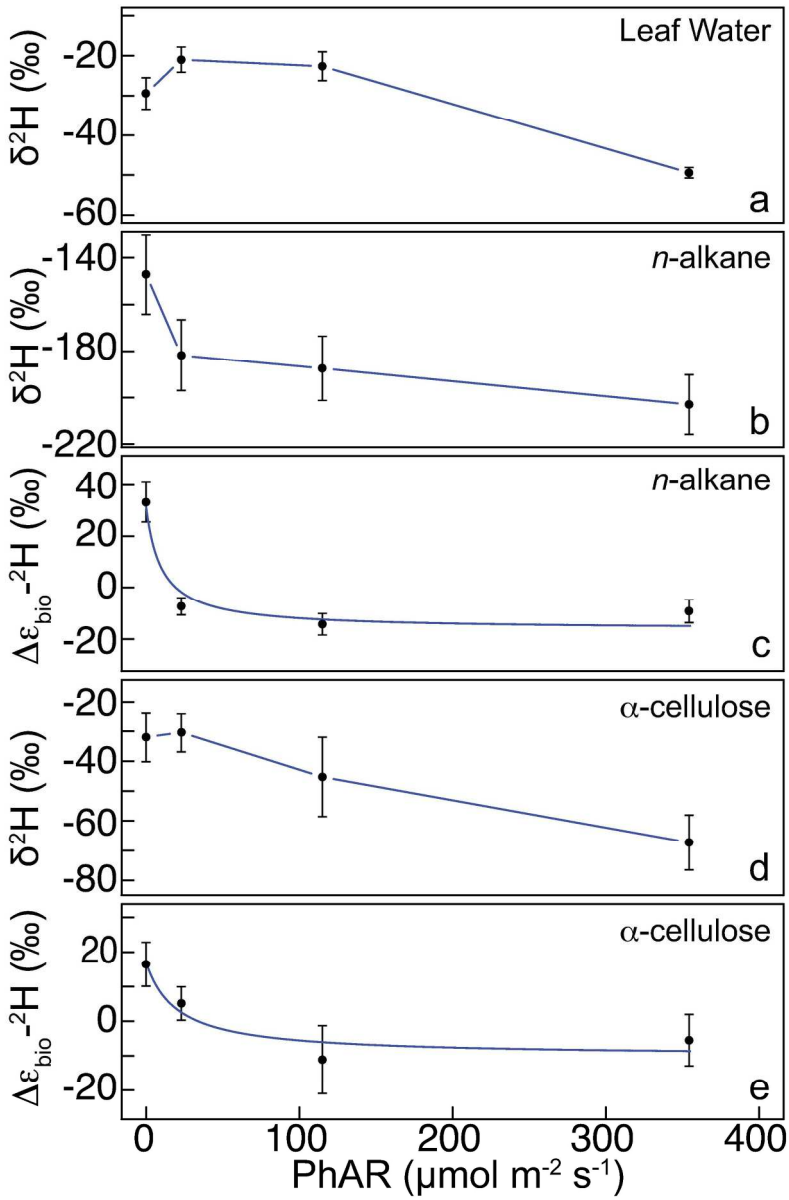

Fig. 3. Leaf water, α-cellulose, *n*-alkane δ^2H values and the corresponding relative ^2H-ε_{bio} for α-cellulose and *n*-alkanes under different light intensities (photosynthetic active radiation, PhAR) averaged across all six species. The magnitude of ^2H-ε_{bio} can differ largely across different species. To allow the comparison of treatment effects on ^2H-ε_{bio} across all six species we standardized the ^2H-ε_{bio} response of a species to the light treatment around its overall mean ^2H-ε_{bio} in the experiment (i.e. Δ^2H-ε_{bio}). Each point corresponds to the averaged values 6 different species (n=6) grown in 3 replicates from the tuber or roots under the different light intensity. The ^2H-ε_{bio} curves for individual species are available of Fig. S2.

176x250mm (300 x 300 DPI)

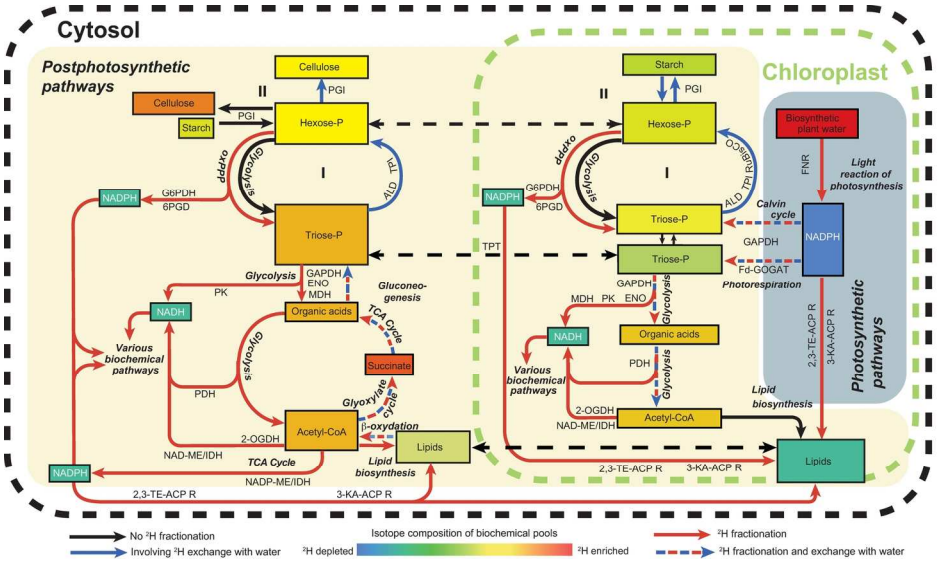

Fig. 4. Schematic view of H flow during processes leading to *n*-alkanes and α-cellulose ^{2}H-ε_{bio}. The key enzymes and pathways responsible for H flow are indicated by their following abbreviations and are based on known biochemical pathways (Rose & Rieder, 1958; Rieder & Rose, 1959; Knowles & Albery, 1977; Cheesbrough & Kolattukudy, 1984; Schleucher et al., 1999; Heldt et al., 2005; Augusti et al., 2006; Zhang et al., 2009; Schirmer et al., 2010; Voet & Voet, 2011; Buchanan et al., 2015; Ehlers et al., 2015). The Roman numerals indicate the two main post-photosynthetic biochemical processes that we suggest to be responsible for the general ^{2}H-enrichment of plant metabolites under low photosynthetic carbohydrate supply: 2-OGDH, 2-oxoglutarate dehydrogenase; 6PGD, 6-phosphogluconate dehydrogenase; ACP, acyl-carrier-protein; ALD, aldolase; ENO, enolase; Fd-GOGAT, ferredoxin glutamine:oxoglutarate aminotransferase; FNR, ferredoxin-$NADP^{+}$ reductase; G6PDH, glucose-6-phosphate dehydrogenase; GAP, glyceraldehyde 3-phosphate; GAPDH, glyceraldehyde 3-phosphate dehydrogenase; IDH, isocitrate dehydrogenase; KA, ketoacyl; ME, malic enzyme; NADP, nicotinamide adenine dinucleotide; NADPH, nicotinamide adenine dinucleotide phosphate; ME, malate dehydrogenase; PDH, pyruvate dehydrogenase; PEP, phosphoenolpyruvate; PGI, phosphoglucose isomerase; PK, pyruvate kinase; oxPPP, oxidative pentose phosphate pathway; TPI, triosephosphate isomerase; TE, trans-enoyl; TPT, triose phosphate translocator; R, reductase; RuBisCO, ribulose-1,5-bisphosphate carboxylase/oxygenase. Succinate dehydrogenase also produced $FADH_2$ in the TCA cycle, but is not represented on the scheme.

172x95mm (300 x 300 DPI)

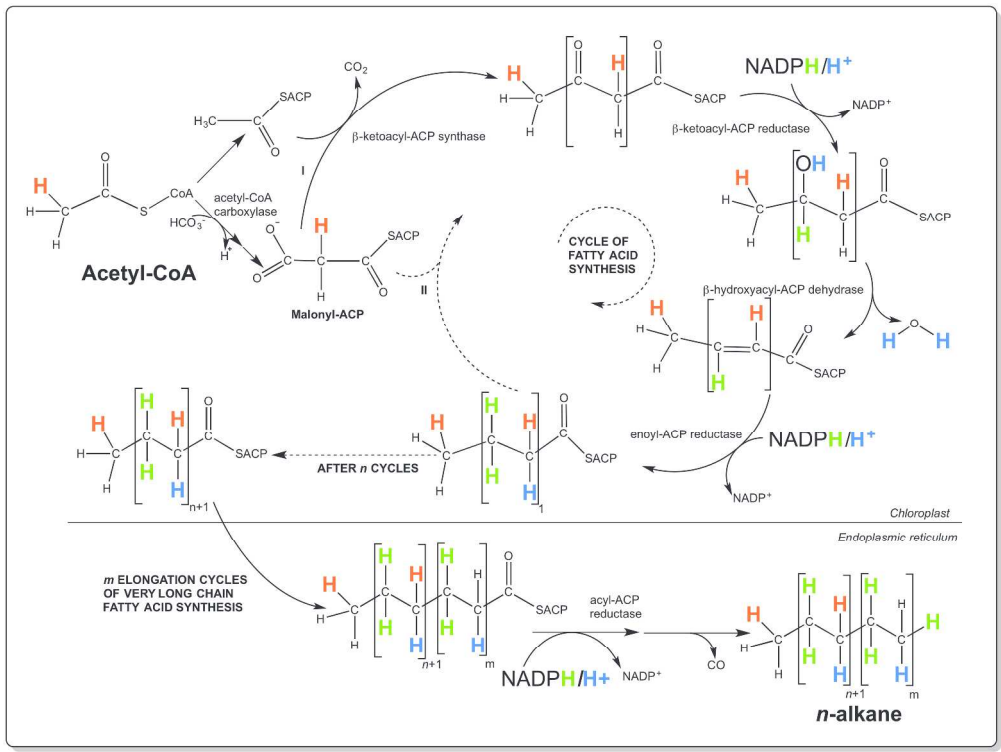

Fig. 5. Simplified view of the biochemical origins of H atoms in *n*-alkane biosynthesis. Black H represent H atoms from the precursor acetyl-CoA. Green H originate from NADPH reduced by the light reaction of photosynthesis in the chloroplast and or by oxPPP and other reactions in the endoplasmic reticulum. Blue H are from H atoms in equilibrium with surrounding water. The fatty acids are generally elongated until 16 or 18 Cs long in the chloroplast and until 32 Cs long in the endoplasmic reticulum; this might also imply different H sourcing (Cheesbrough & Kolattukudy, 1984; Zhang et al., 2009; Schirmer et al., 2010; Buchanan et al., 2015). The red H represent the ^{2}H-depleted atoms that can come from the 3-phosphoglycerate produced upon the photosynthetic C oxidation. In a C29-alkane, of 60 H atoms, 28 comes from NADPH, 14 from water, 17 from manolyl-ACP (which ultimately derives from acetyl-CoA and pyruvate).

298x223mm (300 x 300 DPI)